Proceedings of ASME Turbo Expo 2012
GT2012
June 11-15, 2012, Copenhagen, Denmark

GT2012-68585

SMART POLYGENERATION GRID: A NEW EXPERIMENTAL FACILITY

Mario L. Ferrari **Matteo Pascenti**

Alberto Traverso **Massimo Rivarolo**

mario.ferrari@unige.it
Thermochemical Power Group (TPG) – DIME
University of Genoa, Genoa, Italy

ABSTRACT

This paper presents the development of a new experimental facility for analysis and optimization activities on smart polygeneration grids. The test rig is being designed and built in the framework of the European project "Energy-Hub for residential and commercial districts and transport" (E-HUB), which targets optimal energy management of residential and commercial districts.

The experimental rig, named "Energy aNd Efficiency Research Demonstration District" (E-NERDD), is located inside the University campus in Savona, and is based on four different prime movers able to produce both electrical and thermal energy: a 100 kWe micro gas turbine, a 20 kWe internal combustion engine, a 3 kWe Stirling engine, and a 450 kWe fuel cell/gas turbine hybrid system emulator based on the coupling of a micro gas turbine with a modular vessel. While the electrical side is based on the connection with the campus grid (further developments are planned for a local electrical grid including storage units), thermal energy is managed through a dual ring-based water distribution system. The facility is also equipped with thermal storage tanks and fan cooler units to study and optimize different thermal management algorithms generating different thermal load demands. The facility also includes an absorption chiller for cold water generation. As a result, trigeneration operation is possible in a physically simulated urban district. Moreover, the rig is equipped with six photovoltaic panels (significant for the electrical aspects) and 10 kWp of thermal solar panels to be integrated in the grid.

Further technologies to be considered for the E-NERDD are power plants based on other renewable resource (e.g. with biomass fuel). These systems are planned to be analyzed through real plants (remote connection with the field) or through virtual models based on real-time dynamic approaches.

Experimental tests related to the performance of the micro gas turbine are reported and discussed in this paper. The focus here is on machine correction curves essential to evaluate factors for quantifying ambient temperature influence on machine performance. This analysis is essential for setting the thermal distribution grid and for future optimization tests.

INTRODUCTION

Since power plant technology is the main source of greenhouse gas emissions [1], this industrial field should be carefully considered for future sustainable development. Specifically, to achieve Kyoto Protocol targets [2,3], several efforts are necessary:

- energy saving at the user level [4] (e.g. high efficiency buildings and devices);
- wide development of renewable energy based generation [5];
- innovative emission removal systems [6] (e.g. CO_2 sequestration [7]);
- efficiency improvements at the generation level (e.g. with fuel cell systems [8]).

One significant solution to pursue the emission targets may be obtained by development of a distributed generation paradigm based on smart polygeneration grids able to produce electricity and both heating and cooling thermal power close to

consumers. This is a major revolution for power plant technology from the current centralized generation paradigm that is based on electricity produced by large generation facilities [9] and transferred though transmission and distribution grids to the end consumers.

Several studies [10-12] were carried out to show some disadvantages of centralized generation approach and to justify distributed generation development for future electricity markets. The main drawbacks of the current centralized paradigm are:

- Transmission and distribution cost: about 30% of the costs related to electricity supply is due to this aspect.
- Line and conversion losses: it was evaluated (e.g. in [13]) that about the 6% of produced energy is lost in lines and conversion devices increasing costs and emissions.
- Rural connection: connection of remote areas generates high capital costs and energy losses for long distances to be wired with overhead facilities.
- Investments in grid facilities: The World Energy Investment Outlook 2003 [14] by the IEA showed that more than $16 trillion needs to be invested in energy supply infrastructure worldwide over the period 2001-2030 to meet planned growth in energy demand. The distributed generation approach is a potential solution to reduce these costs.
- Energy efficiency: since the 1960s, the marginal gains in energy efficiency through size increases and use of higher temperatures and pressures started to decrease [15]. In this scenario, cogeneration is the easiest approach to generate a significant additional increase in equivalent efficiency values (electrical and thermal power) of up to 90%. However, it is important to highlight that, since thermal energy is less easily transported than electricity, distributed generation approach (production close to users) is essential.

Moreover, distributed generation, in comparison with centralized energy paradigm, is supported by the following main advantages:

- Security and reliability: distributed generation can contribute to energy security through fuel diversification aspects [16] (for instance, distributed generation can be used at landfill sites to generate energy from biogas) and backup devices (local grids may acts as backups in case of failures).
- Electricity deregulation: in a deregulated electricity market, reserve margin decreases or generator failures can lead to capacity shortfalls. Large electricity consumers can develop acquired distributed generation capacities to avoid these problems.
- Environmental impact: distributed generation is also essential to mitigate the impact of emissions associated with transmission and distribution losses. A general efficiency increase through cogeneration and distributed renewable energy decreases pollution. However, the electrical efficiency is influenced by size and technology type.

These main aspects increase the interest of researchers on distributed polygeneration grids at both industrial and academic levels. Specifically, the Thermochemical Power Group (TPG) of the University of Genoa is involved in a four years European Collaborative project called E-HUB (Energy-HUB for residential and commercial districts and transport) [17]. An e-hub is a physical junction where energy and information streams are interconnected. Moreover, in an e-hub, the different forms of energy can be converted and/or can be stored. Consumers and suppliers of energy are connected to this system through bi-directional energy grids (heating grid, cooling grid, electrical grid (AC and/or DC), gas grid (H_2, biogas, syngas)). It is important to note that a distributed energy generation approach is essential in this concept [18]. This implies that grids exchange energy between different players (e.g. households, renewable energy plants, offices), behaving as energy consumers at one time, and suppliers at another time. Moreover, consumers and suppliers exchange information on their energy needs and/or generation with the e-hub. An important point to be highlighted for these smart grids regards efficiency. For a wide development of these new concepts, it is essential that the e-hub distributes the available energy in the most efficient way to the consumers [18].

In the framework of this project the TPG developed at Savona a new experimental facility for analyses and optimization activities on smart polygeneration grids. This test rig, named "Energy aNd Efficiency Research Demonstration District" (E-NERDD), is based on different prime movers connected to the campus electrical grid and to thermal energy grids (both heating and cooling energy) equipped with vessels for storage technology emulation.

This energy network will integrate data from real components (local-hardware) with virtual as well as remote hardware such as:

- Local-hardware (i.e. real plants located in the laboratory at the Savona campus: a 100 kW recuperated micro gas turbine, a 20 kWe internal combustion engine, a 3 kWe Stirling engine, a 450 kWe hybrid system emulator rig [19], a tri-generation plant based on a water/lithium bromide absorption cooler, a 10 kWp solar thermal system and a 1.1 kWp photovoltaic plant);
- Remote-hardware (i.e. real operating plants offering real data sets through remote connection: a 1 MW operational biogas ICE-CHP plant, three district heating plants fed by local forest biomass [20]);
- Virtual-hardware (i.e. simulated systems using real-time approaches [21]).

The ultimate objective of this experimental facility, named E-NERDD, is the complete emulation of a district equipped

with different distributed generator units and with thermal energy grids. The experimental work will be carried out (inside the E-HUB project) to optimize [22] generation efficiency delineating control logics for energy management. Specifically, starting with load profiles (thermal and electrical), fuel cost, operation cost and machine performance, it will be possible to test and optimize operational logics (i.e. which machines have to operate to satisfy load demand at the highest efficiency conditions [23]) with a laboratory scale real distributed generation district. In comparison with state-of-the-art works [10-13], this facility allows to consider several generation technologies with the high control flexibility of a laboratory, including innovative devices (e.g. hybrid systems) and renewable sources.

Great attention is devoted on experimental results for the ambient temperature correction curves on the 100 kWe turbine. This is an innovative aspect because published experimental wide campaigns on this subject are poor, probably for company data protection reasons. Moreover, this curve evaluation will be essential for future tests on the thermal distribution grid, especially for optimization activities.

NOMENCLATURE

AC	Alternate Current
CHP	Combined Heat and Power
DC	Direct Current
Ex	Exchanger
ICE	Internal Combustion Engine
IEA	International Energy Agency
IP	Internet Protocol address
ISO	International Organization for Standardization
LPG	Liquefied Petroleum Gas
mGT	micro Gas Turbine
PI	Proportional Integral controller
PH	Power and Heat
SOFC	Solid Oxide Fuel Cell
TCP	Transmission Control Protocol
UDP	User Datagram Protocol
WHEx	Water Heat Exchanger
Variables	
COP	Coefficient Of Performance
K_F, K_P, K_T	Coefficient for Eqs.2,4,6
LHV	Low Heating Value [J/kg]
MF	fuel mass flow rate [kg/s]
N	rotational speed [rpm]
P	power [W]
PA1	compressor inlet pressure [Pa]
T	temperature [K]
TA1	compressor inlet temperature [K]
TIT	Turbine Inlet Temperature [K]
TOT	Turbine Outlet Temperature [K]
x,y	General variables (Figs.11-13)
Greek symbols	
η	machine efficiency
Subscripts	
el	electrical
ISO	International Organization for Standardization
max	maximum
nom	nominal
th	thermal

PRIME MOVERS (LOCAL HARDWARE) FOR THE RIG

As already stated in the introduction, different prime movers were installed in the TPG's laboratory for the E-NERDD development (Fig.1 highlights the new components necessary for E-HUB project: the existing facilities are shown not highlighted). They are based on different kinds of technology mainly able to produce (if possible) both electrical and thermal energy.

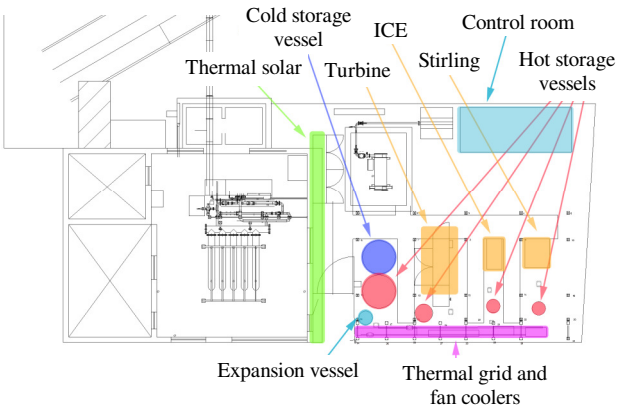

Figure 1. Laboratory plant layout.

100 kWe Recuperated Micro Gas Turbine

This machine is a Turbec T100 PH Series 3 [25] fuelled by natural gas. It is equipped to operate connected to the campus electrical grid. This commercial unit consists of a power generation module (100 kW of electrical power at nominal conditions), a heat exchanger located downstream of the recuperator outlet (hot side) for co-generative applications.

The power module is composed of a single shaft radial machine (compressor, turbine, synchronous generator) operating at a nominal rotational speed of 70000 rpm and a TIT of 950°C (1223.15 K), a natural gas fed combustor, a primary-surface recuperator, a power electronic unit, an automatic control system interfaced with the machine control panel and the auxiliaries (further machine details are shown in Tab.1). In this grid-connected mode, the controller works at constant turbine outlet temperature (TOT). So, the control system changes the fuel mass flow rate to maintain the machine TOT (in steady-state condition) at 645°C (918.15 K). However, the power electronic system allows to generate a 50 Hz current output (at each load values), starting from the high-frequency power (~1167 Hz at full load) from the electrical generator.

Table 1. Details of Micro Gas Turbine.

Net electrical output	100 kW
Net electrical efficiency	30%
Nominal rotational speed	70000 rpm
Nominal TOT	645°C (918.15 K)
Net thermal power	155 kW
Net total efficiency	77%

20 kWe Internal Combustion Engine

The internal combustion engine (ICE) is a TANDEM T20 manufactured by Energia Nova, fuelled by natural gas (20 kW of electrical power at nominal conditions). It is composed of a four-stroke FIRE – 8V 1.2 CNG KY04 engine, working on the Otto cycle basis, coupled with a four-fluid (exhausts, lubricating oil, cooling fluid and water for cogeneration) heat exchanger for hot water production (47.5 kW of thermal power at nominal conditions). The main details related to this prime mover are shown in Tab.2.

Table 2. Internal combustion engine specifications.

Engine	
Cylinder volume	1242 cm^3
Number of cylinders	4
Valves per cylinder	2
Bore x stroke	70.8 x 78.8 mm
Compression ratio	9.8
Rotational speed	3000 rpm
Fuel	Gas (methane, LPG, biogas)
Weight	76 kg
Cogeneration hydraulic circuit	
Nominal water mass flow	3600 l/h
Maximum inlet temperature	74°C (347.15 K)
Maximum outlet temperature	85°C (358.15 K)
Maximum pressure loss	70 kPa
Powers and efficiencies	
Inlet nominal power	70 kW
Electrical nominal power	20 kW
Thermal nominal power	47.5 kW
Electrical nominal efficiency	29%
Natural gas mass flow (CH_4)	≈7.4 Nm^3/h

3 kWe Stirling Engine

The Stirling engine is a GENOA03 manufactured by Genoastirling to be fuelled by biomass (3 kW of electrical power at nominal conditions). It is composed of a pellet burner coupled with a type γ Stirling engine (Fig.2) followed by a heat exchanger for hot water generation.

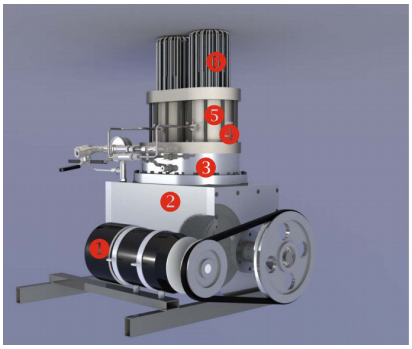

1. Electrical generator
2. Carter
3. Engine block
4. Cooler
5. Recuperator
6. Hot side heat exchanger

Figure 2. Stirling engine picture (courtesy of Genoastirling).

The main details related to this prime mover are shown in Tab.3. However, the cycle efficiency is not specified because, since it is an experimental machine, it has to be evaluated with experiments.

Table 3. Details for the Stirling engine.

Mechanical specifications	
Cylinder volume	880 cm^3
Number of cylinders	2
Working fluid	Air or helium
Maximum pressure	25 bar
Start-up temperature (hot side)	520°C (793.15 K)
Nominal temperature (hot side)	750°C (1023.15 K)
Nominal rotational speed	600 rpm
Electrical nominal power	3 kW
Thermal nominal power	25-30 kW

450 kWe Hybrid System Emulator

The hybrid system emulator test rig [19] is composed of a commercial recuperated micro gas turbine (mGT) [24] and a fuel cell system emulator. This latter facility [25] is based on a cathodic side modular vessel [25], located between the recuperator outlet and the combustion chamber inlet, and an anodic circuit [26].

The machine is a second Turbec T100 PH Series 3 [24] able to produce nominal electrical power of 100 kW (see the related paragraph for details). Moreover, this machine is equipped to operate in stand-alone configuration (control system works at constant rotational speed [19]). This commercial power generator was modified for the coupling with the fuel cell emulator, as described in [25].

The modular cathodic vessel was designed to emulate different fuel cell sizes and technologies [19]. It is composed of two collector pipes, connected at the recuperator outlet and the combustor inlet respectively, and four module pipes connected to both collectors. The maximum volume refers to an SOFC size of about 380 kW (see [26] for design details) and it is equal to about 3.2 m^3.

The anodic recirculation system is composed of a compressed air line (for fuel flow emulation), an anodic single stage ejector [27], and an anodic vessel for a volume of about 0.8 m^3. To better emulate the anodic side, it is necessary to heat up the flow in the anodic loop. For this reason, a pipe-based heat exchanger was developed as shown in [26] (part of the anodic loop was inserted into the cathodic volume to partially heat the anodic flow).

Moreover, this plant was equipped with a steam generator system to inject super-heated steam immediately upstream of the machine combustor [28]. Since it is not possible to re-generate the actual SOFC [29] outlet composition with just steam injection, this new system is essential to operate the test rig at specific chemical composition similitude condition. This steam injection system includes a steam generator, a pre-superheater and a superheater. This last component is necessary to increase the steam temperature from the steam generator outlet condition to a temperature suitable for the turbine combustor inlet (around 515°C: 788.15 K). Further details on plant layout and the most recent results are shown in [28].

To complete the emulation of an SOFC hybrid system a real-time model was developed in Matlab®-Simulink® to couple with the experimental test rig. This model (developed with components validated in previous works [21]) was based on the simplification of simulation components (cell stack, reformer, anodic loop, off gas burner, expander) developed in the TRANSEO tool [30] of the TPG research group. Through the Real-Time Windows Target tool and the UDP interface approach, it was possible to study the entire hybrid system using the model for components not physically present in the test rig [30]. Further details on plant layout and on emulation tests are shown in [30] (for the sake of brevity, no additional information on this emulator is reported here; furthermore, several works [19,25-26,28-29] completely devoted to this test rig are shown).

Tri-Generation Plant

To carry out tests at compressor inlet temperature values under 20°C (293.15 K) and to study tri-generative configurations, the hybrid system emulator was equipped with an absorption cooler. This device makes use of the thermal content of the machine exhaust flow (an exhaust/water heat exchanger can produce up to about 155 kW of thermal power: water at 95°C, which means 368.15 K) to obtain cold water (7-12°C, which means 280.15-285.15 K). This refrigeration energy is essential for the machine inlet and for the laboratory cooling during summer or long time tests.

The cooler is designed to produce up to 102 kW of cooling power. This system is based on an absorption inverse cycle (water/lithium bromide) operating at a 0.75 nominal COP value. The plant is also equipped with a fan cooler to emulate a heating system operating in tri-generative condition. So, while the fan cooler is used to emulate a heating system, the heat exchangers used to manage the cold power are essential to emulate a cold thermal load.

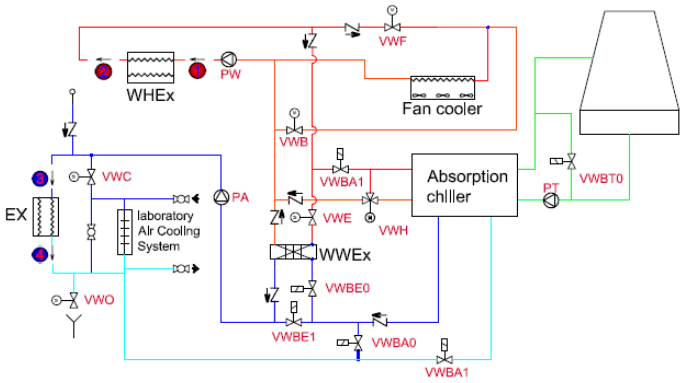

Figure 3. Water system plant diagram for the tests with absorption cooler.

Figure 3 shows the plant diagram related to cold water generation (from the absorption cooler) and thermal power management. In Fig.3, the heat exchanger used to generate hot water from the turbine exhausts is called "WHEx" and the "Ex" exchanger refers to the devices installed for controlling compressor inlet temperature through both cold or hot water. This plant is also equipped with a 260 kW evaporative tower for water refrigeration. Moreover, to generate heating conditions at the compressor inlet level (for instance for the emulation of a summer performance during winter) a water/water heat exchanger was included.

10 kWp Solar Thermal System

The solar thermal system is based on five 2 m^2 flat panels of 2 kW (peak power), manufactured by SunHeat. These panels are located close to the southern exterior wall of the laboratory building with a 20° inclination from the vertical direction. They are based on a copper absorbing plate manufactured with a selective TINOX material to obtain a 95% absorbing coefficient [31] and include high fidelity components: anodized aluminum support, anti-hail hardened glass, ultrasound welded pipes, anti-ultraviolet gaskets, and rock wool thermal insulation (high thickness). The circulation group is equipped with a pump, a 24 l expansion vessel, a safety valve, a control unit with temperature probes, a thermostatic mixer and connection pipes (the five panels are connected in series).

1.1 kWp Photovoltaic Plant

The photovoltaic plant installed in the laboratory is based on six LX-185 M panels manufactured by Luxor Solar. The main details related to the basic unit for this prime mover are shown in Tab.4.

Table 4. Single panel details of the photovoltaic plant.

Electrical data	
Nominal peak power	185 W
Nominal peak current	5.14 A
Nominal voltage	36 V
Short circuit current	5.62 A
Open circuit voltage	43.58 V
Panel efficiency	14.50%
Technical data	
Panel type	Single-crystal silicon
Cell number	72 (6 x 12)
Cell dimension	125 x 125 mm
Panel dimension (a*l*h)	1580 x 808 x 35 mm

The six panels are connected in series to an inverter. This electrical component is essential to convert (with 90.9% efficiency) the DC current (from photovoltaic plant) to the 50 Hz AC electrical grid.

PRIME MOVERS (OTHER HARDWARE) FOR THE RIG

Other power plants may be considered for technology not directly installed at TPG laboratory.

Remote Hardware

The main additional systems are remote power plants connected with the laboratory through an internet connection. For this reason the acquisition/control system will include appropriate TCP/IP interface to receive data from remote hardware and to send essential control issues.

The first plant to be considered here is a biomass anaerobic digestion plant (animal manure, silo corn, agricultural residues) for about 1 MWe power, equipped with heat generation exchangers and located in Italy (Val Pesio).

In addition, other plants to be operated through a remote connection are three thermal biomass plants [20] located in the villages of Campo Ligure, Rossiglione and Masone (in the Genoa hinterland). The plants of Campo Ligure and Rossiglione are equipped with boilers of 0.7 MWth and 1.1 MWth, respectively; in Masone a burner of 1.1 MWth was installed.

Virtual Hardware

For the technology not considered here (e.g. wind power plants), real-time models will be coupled to the experimental rig. These will be simple models based on "black box" approaches (e.g. interpolation between performance curves) probably based on Matlab®-Simulink® visual interface. For instance, for a wind plant, it will be possible to include in the optimization tests the electrical power produced by this technology. The model will provide the generation characteristics from ambient conditions and machine performance curves. No further details are included here because development of these virtual hardware devices are planned in a future task of the E-HUB project.

PLANT LAYOUT OF THERMAL GRIDS

Two different piping philosophies were developed at the laboratory for distribution of both heating and cooling powers. Both thermal grids are used to carry out emulation tests for optimization of districts based on distributed generation approach. For this reason, the laboratory is equipped with several fan coolers, driven by inverters, able to generate thermal demand profiles similar to loads driving real plants. A new water distribution grid was designed for the thermal heating energy of four different prime movers (the unmodified turbine, the internal combustion engine, the Stirling engine and the solar thermal panels). On the other hand, the cooling piping layout is based on the layout shown in Fig.3 (the rig was modified specifically for the coupling with a storage vessel).

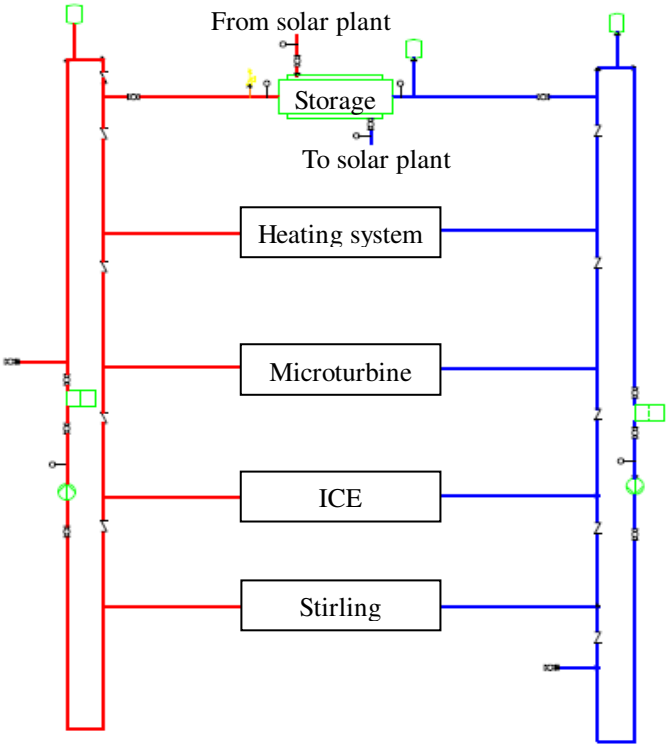

Figure 4. Heating distribution grid.

Heating Distribution Grid

This pipe grid is based on two water distribution rings (Fig.4). The design temperature values are: 80°C (353.15 K) for the high temperature ring (red color in Fig.4) and 50°C (323.15 K) for the other pipe line (blue color in Fig.4). Generators are connected in parallel feeding the high temperature ring. Low temperature ring is used to feed water to the generators (turbine, ICE and Stirling engine). The users ("Heating system" in Fig.4 and emulated in the rig by a large

variable speed fan cooler: 300 kW maximum thermal power) are connected to the rings as the generators. They receive water from the high temperature ring and deliver cold water (after heating) to the other ring. A large vessel (5000 l) is connected between the rings to compensate the power mismatch between generators and users and to store thermal energy. This device was designed to have a high flexibility for the tests also considering standard vessel sizes. When it is fully charged it allows to sustain a 150 kW thermal load for at least one hour with all prime movers off. A size optimization will be carried out during the test campaigns. This vessel includes a coil for the connection with the 10 kWp solar thermal system. With this piping philosophy and with a large temperature difference between the rings (e.g. 30 K) it is possible to develop large scale distribution grids without large mass flow rate values in the rings. Moreover, this configuration can guarantee the same temperature values for all the buildings. On the ring side it is not necessary to use expensive pumps because low scale mass flow rate values are enough to guarantee uniform temperature values.

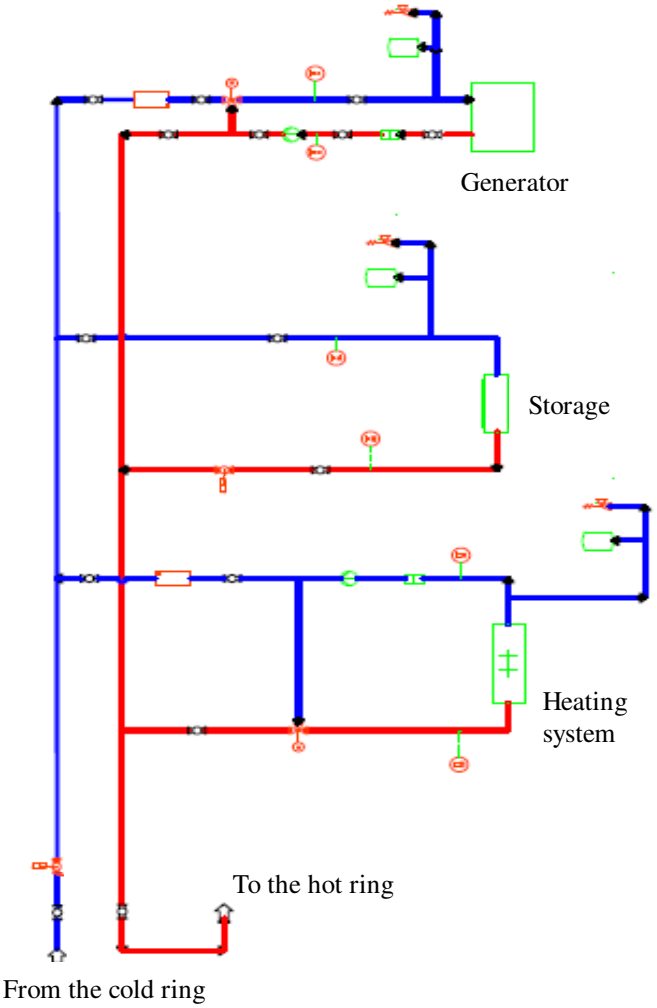

Figure 5. Generator block details.

This layout is a cheap solution for large distribution grids because large mass flow rates are not required. Also, this configuration is not affected by the technological problems (due to the temperature of delivered water) shown by single ring distribution grids. The only disadvantage of this configuration is related to the lack of complete separation between generator flows and water flows delivered to users. For this reason, if this separation is necessary a water/water heat exchanger has to be included.

Since each district building equipped by a generator may include a local heating system and local storage devices, each generator block (e.g. the turbine) in Fig.4 includes a complex layout. This approach was chosen to provide the highest flexibility to the rig for tests related to optimization of polygeneration grids.

To show details related to the generator blocks Fig.5 is an example of possible components located inside a building equipped with thermal heating devices, a prime mover and a local thermal storage. Figure 5 is a general scheme showing layout details of the main generator circuits: the microturbine, the ICE and the Stirling engine. The thermal power produced by the generator may be used locally (the "Heating system" of Fig.5) or delivered to the grid. On the other hand, local users (emulated in the rig by a variable speed fan cooler) may exploit thermal power from the rings when local generator is off or is producing too low thermal power. The maximum power values related to these fan coolers are: 160 kW for the turbine, 60 kW for the ICE , 35 kW for the Stirling engine. The local vessel may be used to store thermal power not immediately consumed locally and available when necessary. The size of these storage volumes, designed to have a significant local thermal endurance considering available space, are: 1000 l for the turbine, 500 l for the ICE , 500 l for the Stirling engine. Each generator block is equipped with two constant speed electrical pumps able to ensure the design flows inside the components. The temperature values are controlled by three-way valves able to maintain, including part-load conditions, 80°C (353.15 K) at the generator outlet and 50°C (323.15 K) at the fan cooler outlet. For this reason, PI controllers are implemented in the control/acquisition system (developed in LabVIEW^{TM}) for managing these three-way valves (one PI controller for each valve). In addition, the rig is equipped by on/off valves to switch from one configuration (e.g. generator is producing heat for the local user and ring connection is closed) to another (e.g. the rings are feeding the local user and local generator is off).

Cooling Distribution Grid

The cooling distribution grid is extremely simple because it is based on the existing layout shown in Fig.3. For the development of this polygeneration grid a 5000 l storage vessel (sized with the same approach used for the heating storage device) is also included for the cold water produced by the absorption cooler. The "Users" of Fig.6 are the heat

exchangers for cooling the T100 intake and the internal part of the laboratory (see Fig.3). As shown in Fig.6 it is possible to define four operating configurations managed by a set of on/off valves:

1. The absorption cooler is working and the vessel is excluded (1,2,5,8,10 valves open; 3,4,6,7,9 valves closed). In this case the cooler is directly connected to the users.
2. The absorption cooler is working and the users are excluded (1,2,4,7,8,10 valves open; 3,5,6,9 valves closed). This is the storage vessel charging mode.
3. The absorption cooler is working and both lines of users and vessel are open (1,2,4,6,8,10 valves open; 3,5,7,9 valves closed). Users are connected in series with the vessel which is able to temporarily satisfy a thermal load higher than cold power produced by the cooler.
4. The cooler is not working and the user demand is satisfied just by the vessel (2,4,6,8,9 valves open; 1,3,5,7,10 valves closed). It is a temporary configuration.

The cooler bypass line (valve 9) can also be opened when it is necessary to exclude the cooler.

Also for this cooling grid a control/acquisition software was developed in LabVIEW™ for managing all the valves and the auxiliary components (e.g. the fan of the cooling tower) necessary for correct operations with the absorption cooler.

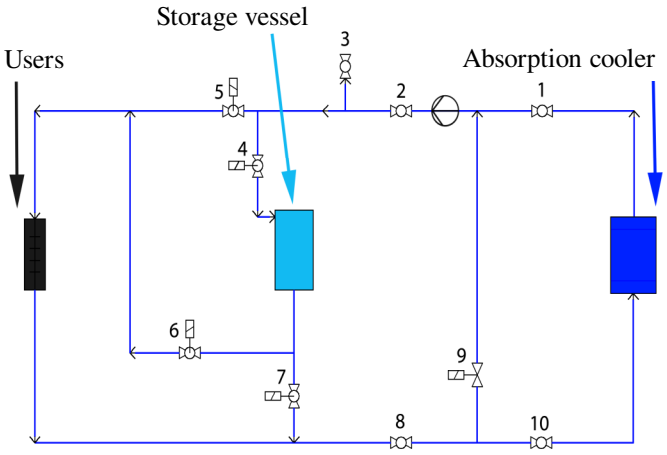

Figure 6. Cooling distribution grid.

PERFORMANCE DATA FOR A GENERATOR: THE T100 MICRO GAS TURBINE

The initial step related to this E-NERDD laboratory refers to tests on the performance of each single generator device. For example, this paper discusses the T100 performance at both design and part-load conditions. The results shown here, even if obtained for a specific machine, can be significant for microturbines with similar size (in the 60-200 kW range of electrical power: errors increase with the size difference increase from the T100 machine and changing technology type). This performance evaluation approach was carried out for other prime movers too, but not reported here for brevity reasons.

In this paper attention is focused on machine correction curves, because of the large influence on machine performance of the compressor inlet temperature [25]. For this reason, a water system (see [25] for further details) equipped with water/air heat exchangers was coupled with the absorption cooler. With this approach it is possible to operate tests at constant compressor inlet temperature in the range 290-310 K during whatever seasons.

Machine Performance Curves

Performance curves were evaluated considering the machine connected to the electrical grid: the control system receives the required electrical power output as input and regulates the fuel mass flow and rotational speed in order to obtain it. Turbine Outlet Temperature (TOT) value is kept constant and equal to its nominal value of 645°C (918.15 K). The minimum electrical power value considered in the experimental campaign is close to 20 kW, corresponding to 75% of nominal rotational speed: lower rotational speed values would determine surge conditions for the compressor and thus should be avoided. The maximum electrical power level is affected by ambient conditions, in particular by ambient temperature (TA1).

Three different test series were carried out considering respectively 290 K, 300 K and 310 K as ambient temperature values: all performance curves were obtained starting from 75% rotational speed condition and increasing it gradually to nominal conditions, considering electrical power steps of 10 kW. The data are reported in the following figures referred to design values shown in Tab.5.

Table 5. Machine reference values for the following figures.

Fuel mass flow rate (MF)	7.2 g/s
Rotational speed	70000 rpm
Net electrical power (P_{el})	100 kW
Turbine outlet temperature	918.15 K
Net thermal power (P_{th})	145 kW

In Fig.7, the rotational speed, referred to its nominal value, is plotted as a function of the electrical net power referred to its nominal value as well: three curves are shown, corresponding to the three ambient temperatures considered. It is essential to note that the minimal rotational speed is equal to 75% of nominal value, to avoid dangerous surge conditions for the compressor.

As can be inferred from Fig.7, in the 290 K curve almost nominal conditions are verified and the maximum electrical

net power can be produced. For the 300 K curve, the maximum electrical power that can be produced is about 92% of nominal value. Furthermore, for the 310 K Fig.7 shows a further power decrease, down to 80% of nominal value.

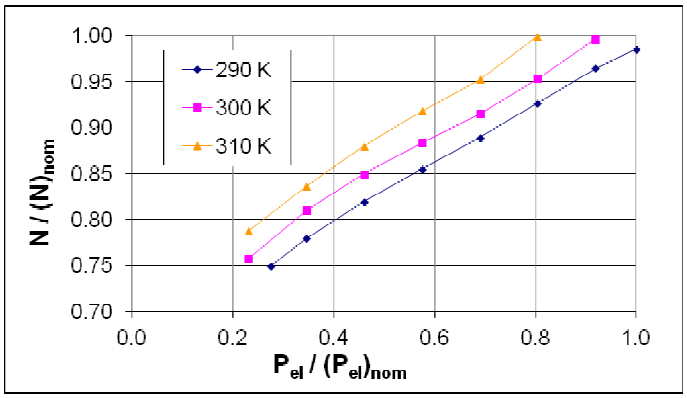

Figure 7. Machine rotational speed ratio.

In Fig.8 the electrical efficiency, as defined in Eq.1, referred to its nominal value, is plotted as a function of electrical net power, with reference to its nominal value: again, three curves are shown. For the 290 K curve, nominal conditions are verified at the full power level. For the 300 K curve, the maximum efficiency is decreased by about 6% from its nominal value; for 310 K curve, efficiency never exceeds the 90% of the nominal value, thus showing the relevant impact of ambient temperature on micro gas turbine performance.

$$\eta = \frac{P_{el}}{MF \cdot LHV} \qquad (1)$$

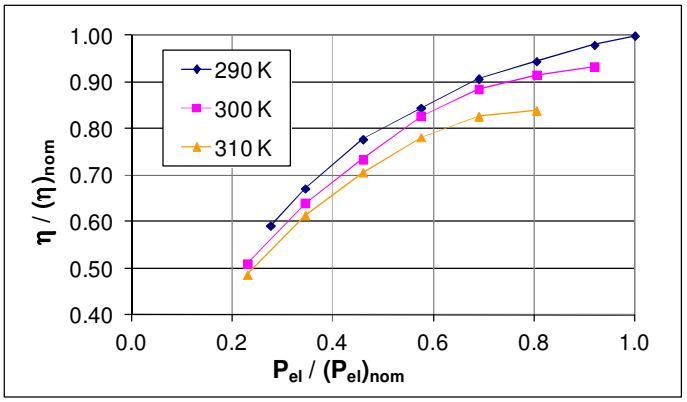

Figure 8. Machine efficiency ratio.

Figure 9 shows fuel mass flow rate referred to its nominal value, plotted as a function of electrical net power, referred to its nominal value: three curves are shown also in this case. For the 290 K curve, nominal conditions are verified at the full power level. Increasing ambient temperature to 300 K and 310 K, fuel consumption increases at equal values of electrical net power; consequently, cycle efficiency decreases, as shown in Fig.9 and as predicted from Eq.1. Also in Fig.9, for 300 K and 310 K curves maximum electrical power decreases and nominal value cannot be reached.

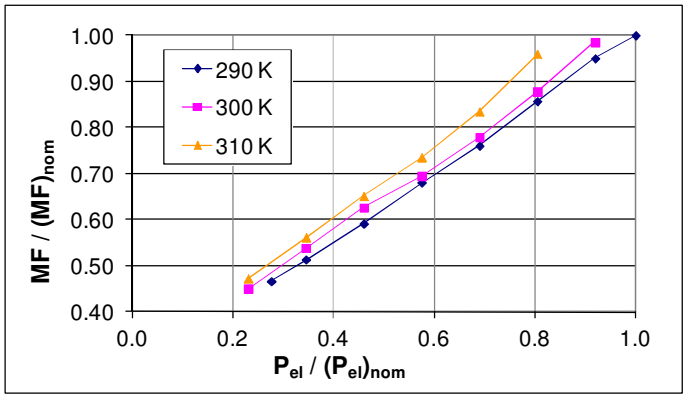

Figure 9. Machine fuel mass flow rate ratio.

Figure 10 shows machine thermal power, plotted as a function of electrical net power, referred to its nominal value: for the 290 K curve, nominal conditions of electrical and thermal power can be reached. Increasing ambient temperature to 295 K and 300 K, thermal power increases and could be higher than its nominal value; on the other hand, nominal electrical net power is not available, consequently cycle efficiency decreases. For this test, the 290-295-300 K ambient temperatures were used instead of 310 K, since the thermal power was measured during more recent tests. Previous experiments showed that the 310 K could cause serious damage to the machine power electronics.

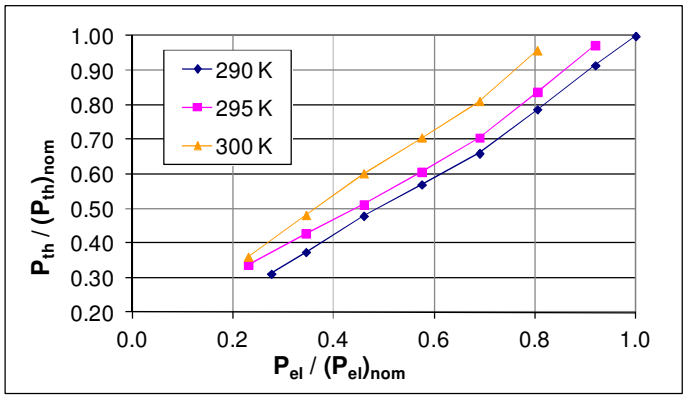

Figure 10. Machine thermal power ratio.

Machine Correction Curves

The results presented were derived from experimental tests performed considering different ambient conditions. In real application, plant commissioning and performance testing are carried out at the current ambient temperature. As a result, performance needs to be corrected to the ISO conditions (288.15 K, 1.013 bar, 60% relative humidity) through

correction curves normally provided by the supplier. The power output of the whole gas turbine cycle is influenced by various parameters, the most important ones being:

1. ***Ambient temperature:*** ambient temperature has an influence on the gas turbine output, since its increase will determine an efficiency decrease; a value of 290 K is assumed as the reference value, because tests were carried out at 290 K not at 288.15 K.
2. ***Ambient pressure:*** ambient pressure affects the gas turbine compressor air flow and therefore the gas turbine power outlet; a reference value of 1.013 bar is assumed. However, once the installation site is determined and nominal operating conditions defined, pressure does not vary significantly along the year, so its influence can be neglected compared to ambient temperature.
3. ***Air humidity:*** the air humidity has some influence on gas turbine output; a relative humidity of 60% is assumed as reference value. However its variation has a negligible effect on the cycle, compared to ambient temperature.

Since the influence of ambient pressure and air humidity is negligible, compared to ambient temperature influence, only the latter was considered relevant to correct the micro gas turbine power and heat outputs, as well as fuel consumption.

In order to quantify ambient temperature influence on machine performance, correction factors were defined: these allow the user to determine machine performance in several working conditions, taking into account the actual ambient temperature, usually different from the reference value.

In Fig.11, fuel consumption, referred to fuel consumption at ISO conditions, is plotted versus the temperature variation from the 290 K reference value: the blue line represents the average value of measured values, with ambient temperatures of 290 K, 300 K and 310 K respectively. To interpolate and extrapolate the experimental results, a linear approximation has been used, as it follows:

$$\frac{MF}{MF_{ISO}} = 1 + K_F * \Delta T \qquad (2)$$

K_F represents the correction factor for fuel consumption, whose value determines the relationship between ambient temperature and fuel consumption variation. A linear relationship from measured values was found for this particular case with correction factor value equal to 0.0047; thus, Eq.2 can be written as Eq.3.

$$\frac{MF}{MF_{ISO}} = 1 + 0.0047 * \Delta T \qquad (3)$$

In Fig.12, the ambient temperature influence on maximum net electrical power, referred to nominal conditions, is plotted. Considering measured values, with ambient temperature of 290 K, 300 K and 310 K respectively, tests show that the maximum electrical power decreases, following the relationship expressed by the linear approximation of Eq.4.

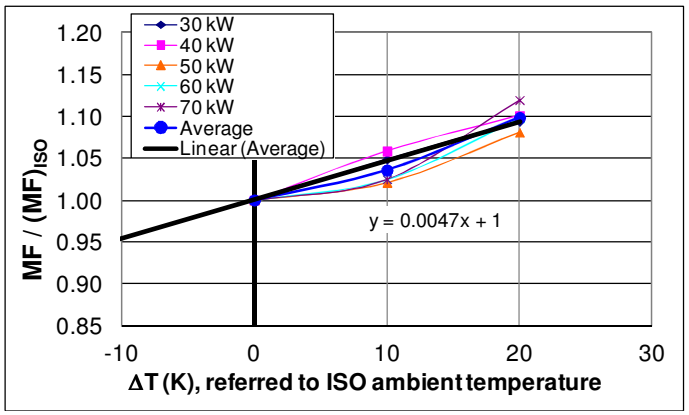

Figure 11. Ambient temperature influence on fuel mass flow rate.

$$\frac{P_{el\,\max}}{P_{el,ISO\,\max}} = 1 + K_P * \Delta T \qquad (4)$$

K_P represents the correction factor for maximum electrical net power, whose value determines the relationship between ambient temperature and maximum electrical power variation: from measured values, a linear relationship is obtained for this particular case and correction factor value is equal to -0.0092. Thus, Eq.4 can be written as Eq.5.

$$\frac{P_{el\,\max}}{P_{el,ISO\,\max}} = 1 - 0.0092 * \Delta T \qquad (5)$$

It should be observed that Eq.5 validity is verified only if ambient temperature increases from reference conditions: vice versa, if ambient temperature gets lower, electrical power is constant, since nominal value cannot be overcome, as determined by the machine control system.

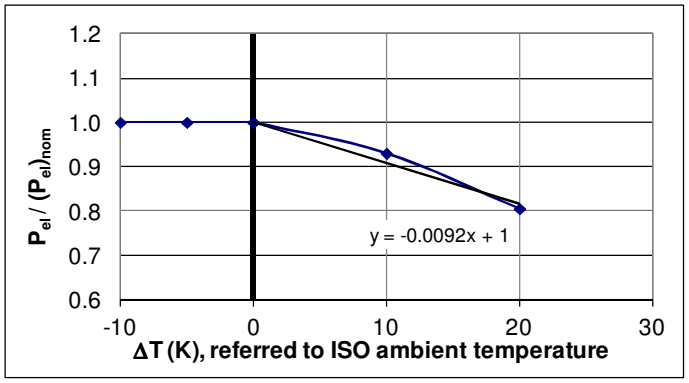

Figure 12. Ambient temperature influence on maximum electrical power.

In Fig.13, the ambient temperature influence on thermal power, referred to nominal conditions, is plotted. Considering measured values, with ambient temperature of 290 K, 295 K

and 300 K respectively, the thermal power increases, following the relationship expressed by the linear approximation of Eq.6.

$$\frac{P_{th}}{P_{th,ISO}} = 1 + K_T * \Delta T \quad (6)$$

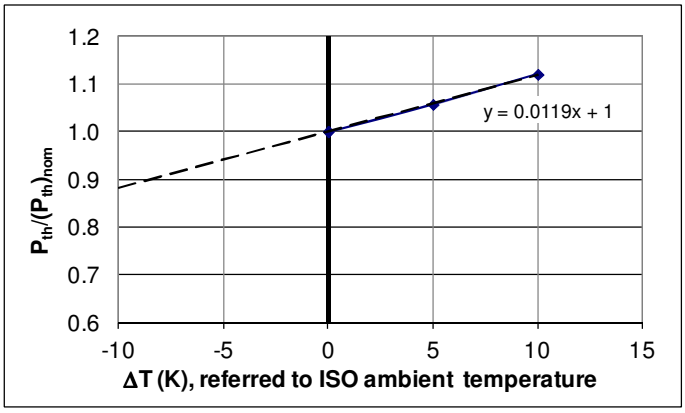

Figure 13. Ambient temperature influence on maximum thermal power.

K_T represents the correction factor for thermal power, whose value determines the relationship between ambient temperature and thermal power variation: from measured values, it was calculated that Eq.6 can be written as Eq.7.

$$\frac{P_{th}}{P_{th,ISO}} = 1 + 0.0119 * \Delta T \quad (7)$$

CONCLUSIONS

A new experimental test rig, named "Energy aNd Efficiency Research Demonstration District" (E-NERDD), was developed at the TPG laboratory of the University of Genoa, Italy. The aim of this facility is experimental analysis and optimization activities on smart polygeneration grids.

The main results related to the rig development presented in this paper are shown in the following points.

- This grid will integrate data from real components (local-hardware) with virtual as well as remote hardware such as:
  - local hardware: a 100 kWe recuperated micro gas turbine, a 20 kWe internal combustion engine, a 3 kWe Stirling engine, a 450 kWe hybrid system emulator rig, a tri-generation plant based on a water/lithium bromide absorption cooler, a 10 kWp solar thermal system and a 1.1 kWp photovoltaic plant;
  - remote hardware: a 1 MW operational biogas ICE-CHP plant, three district heating plants fueled by local forest biomass;
  - for the technology not considered here with real plants (e.g. wind power plants) real-time models will be coupled to the experimental rig.
- The heating distribution grid is based on a two ring layout operated at a 30 K temperature difference: 80°C (353.15 K) for the high temperature ring and 50°C (323.15 K) for the other pipe line.
- The design of this heating system is carefully presented with attention focused on the emulation a general district building equipped by a generator (e.g. the 100 kWe gas turbine). Furthermore, it includes, in the rig, a local heating system and a local storage device.
- The design of the cooling distribution grid is presented focusing attention on the integration of a 5000 l storage vessel with the existing pipes.

The performance tests for the T100 machine are discussed here considering tests operated with the machine connected to the electrical grid at constant compressor inlet temperature in the range 290-310 K. The following points show a performance comparison with the 290 K condition.

- The rotational speed performance curve shows a 4% increase for the maximum electrical power at 300 K and an 7% increase at 310 K.
- The efficiency curves show that for the 300 K test the maximum efficiency is decreased by about 6% from its nominal value, and for 310 K curve efficiency never exceeds the 90% of the nominal value.
- Increasing compressor inlet temperature from 290 K to 310 K, it is possible to note a fuel mass flow increase (at maximum electrical load) of 10% and an average thermal power increase (at maximum electrical load) of 22%.
- The machine correction curves, developed to obtain linear average correlations between temperature variation and properties, show the calculation of the following coefficients (the general correlation is: Property ratio = 1 + Coefficient * ΔT): 0.0047 for the fuel mass flow rate ratio, -0.0092 for the electrical power ratio, and 0.0119 for the thermal power ratio.

As soon as the installation activities related to both thermal grids are completed (including the development of acquisition and control system), the commissioning and preliminary tests will be done. Then, considering the importance of this research field [32,33], an optimization tool [22] by TPG will be coupled to the rig for the experimental campaigns to be carried out in the E-HUB project. In addition, in collaboration with other partners, it will be possible to test different managing logics to be implemented for real district applications.

While all the electrical generators are currently connected to the centralized electrical grid, further developments are planned for a local electrical grid (both DC and AC equipments) including storage units based on battery or supercapacitor technology.

ACKNOWLEDGMENTS

The research leading to these results has received funding from the European Union Seventh Framework Programme under the European Project E-HUB, grant agreement n° 260165.

Additionally, the authors would like to thank the following staff of TPG for their support in the rig development activities: Prof. Aristide F. Massardo, Dr. Loredana Magistri, and Mr. Alessandro Sorce.

REFERENCES

[1] US EPA., 2003, "Inventory of US Greenhouse Gas Emissions and Sinks: 1990–2001". EPA 430-R-03-004. US Environmental Protection Agency, Washington, DC.

[2] Kathib, H., 2004, "Energy Considerations Global Warming Perspectives", World Energy Council. Energy Permanent Monitoring Panel of the World Federation of Sciences.

[3] Quirion, P., 2010, "Complying with the Kyoto Protocol Under Uncertainty: Taxes or Tradable Permits?", Energy Policy, Vol. 38, Issue: 9, pp. 5166-5173.

[4] Dubois, M.C., Blomsterberg, A., 2011, "Energy Saving Potential and Strategies for Electric Lighting in Future North European, Low Energy Office Buildings: a Literature Review", Energy and Buildings, Vol. 43, Issue: 10, pp. 2572-2582.

[5] Arent, D.J., Wise, A., Gelman, R., 2011, "The Status and Prospects of Renewable Energy for Combating Global Warming", Energy Economics, Vol. 33, Issue: 4, pp. 584-593.

[6] Agazzani, A., Massardo, A.F., Frangopoulos, C.A., 1998, "Environmental Influence on the Thermoeconomic Optimization of a Combined Plant with NO_x Abatement", Journal of Engineering for Gas Turbine and Power, Vol. 120, pp.557-565.

[7] Pires, J.C.M., Martins, F.G., Alvim-Ferraz, M.C.M., Simoes, M., 2011, "Recent Developments on Carbon Capture and Storage: an Overview", Chemical Engineering Research & Design, Vol. 89, pp. 1446-1460.

[8] Costamagna, P., Magistri, L., Massardo, A. F., 2001, "Design and Part-load Performance of a Hybrid System Based on a Solid Oxide Fuel Cell Reactor and a Micro Gas Turbine", *Journal of Power Sources*, 96, pp. 352-368.

[9] McDonald, J., 2008, "Adaptive Intelligent Power Systems: Active Distribution Networks", *Energy Policy*, Vol. 36, pp. 4346–4351.

[10] Pepermans, G., Driesen, J., Haeseldonckx, D., Belmans, R., D'Haeseleer, W., 2005, "Distributed Generation: Definition, Benefits and Issues", *Energy Policy*, Vol. 33, pp. 787-798.

[11] Borbely, A.M., Kreider, J.F., 2001, "Distributed Generation: the Power Paradigm for the New Millennium", CRC Press.

[12] Massardo, A.F., 2001, "Cogeneration", John Wiley Encyclopedia of Electronic and Electrical Engineering, New York, J.Webster Ed.

[13] Mendez, V.H., Rivier, J., De La Fuente, J.I, Gomez, T., Arceluz, J., Marin, J., 2002, "Impact of Distributed Generation on Distribution Network". Universidad Pontificia Comillas, Madrid.

[14] Fatih, B., 2003, "World Energy Investment Outlook to 2030", Exploration & Production: The Oil & Gas Review - 2003, Vol. 2, pp. 130-133.

[15] Hirsh, R.F., 1989, "Technology and Transformation in the American Electric Utility Industry", Cambridge University Press, New York.

[16] International Energy Agency, 2002, "Distributed Generation in a Liberalized Energy Market", Jouve, France.

[17] E-HUB European Collaborative Project No. 260162, Annex I, May 2010.

[18] Piacentino, A., Cardona, F., 2008, "An Original Multi-Objective Criterion for the Design of Small Scale Polygeneration Systems Based on Realistic Operating Conditions", Applied Thermal Engineering, Vol. 28, pp. 2391-2404.

[19] Ferrari, M.L., Pascenti, M., Bertone, R., Magistri, L., 2009, "Hybrid Simulation Facility Based on Commercial 100 kWe Micro Gas Turbine", *Journal of Fuel Cell Science and Technology*, Vol. 6, pp. 031008_1-8.

[20] Porta, M., Traverso, A., Marigo, L., 2006, "Thermoeconomic Analysis of a Small-Size Biomass Gasification Plant for Combined Heat and Distributed Power Generation", ASME paper GT2006-90918, ASME Turbo Expo 2006, Barcelona, Spain.

[21] Ghigliazza, F., Traverso, A., Massardo, A.F., Wingate, J., Ferrari, M.L., 2009, "Generic Real-Time Modeling of Solid Oxide Fuel Cell Hybrid Systems", *Journal of Fuel Cell Science and Technology*, Vol. 6, pp. 021312_1-7.

[22] Bozzo, M., Caratozzolo, F., Traverso, A., 2012, "Smart Polygeneration Grid: Control and Optimization System", ASME paper GT2012-68568, ASME Turbo Expo 2012, Copenhagen, Denmark.

[23] Sheikhi, A., Ranjbar, A.M., Oraee, H., Moshari, A., 2011, "Optimal Operation and Size for an Energy Hub with CCHP", *Energy and Power Engineering*, Vol. 3, pp. 641-649.

[24] Turbec T100 Series 3, 2002, "Installation Handbook".

[25] Ferrari, M.L., Pascenti, M., Magistri, L., Massardo, A.F., 2010, "Hybrid System Test Rig: Start-up and

Shutdown Physical Emulation", *Journal of Fuel Cell Science and Technology*, Vol. 7, pp. 021005_1-7.

[26] Ferrari, M.L., Pascenti, M., Magistri, L., Massardo, A.F., 2010, "Analysis of the Interaction Between Cathode and Anode Sides With a Hybrid System Emulator Test Rig", ASME Paper ICEPAG2010-3435, International Colloquium on Environmentally Preferred Advanced Power Generation 2010, Costa Mesa, California, USA.

[27] Ferrari, M.L., Pascenti, M., Massardo, A.F., "Ejector Model for High Temperature Fuel Cell Hybrid Systems: Experimental Validation at Steady-State and Dynamic Conditions", *Journal of Fuel Cell Science and Technology*, Vol. 5, pp. 041005_1-7.

[28] Ferrari, M.L., Pascenti, M., Traverso, A.N., Massardo, A.F., 2011, "Hybrid System Test Rig: Chemical Composition Emulation With Steam Injection", accepted for publication on *Applied Energy*.

[29] Magistri, L., Traverso, A., Massardo, A.F., Shah, R.K., 2006, "Heat Exchangers for Fuel Cell and Hybrid System Applications", *Journal of Fuel Cell Science and Technology*, Vol. 3, pp. 111-118.

[30] Caratozzolo, F., Ferrari, M.L., Traverso, A., Massardo, A.F, 2011, "Real-Time Hardware-in-the-Loop Tool for a Fuel Cell Hybrid System Emulator Test Rig", 5th International Conference on Energy Sustainability & 9th Fuel Cell Science, Engineering and Technology Conference, ASME Paper ESFuelCell2011-54315.

[31] http://www.cordivari.it/prodotti/tech/COLLETTORI_SOLARI.pdf

[32] Wu, Y.J., Rosen, W.A., 1999, "Assessing and Optimizing the Economic and Environmental Impacts of Cogeneration/District Energy Systems Using an Energy Equilibrium Model", *Applied Energy*, Vol. 62, pp. 141-154.

[33] Thorin, E., Brand, H., Weber C., 2005, "Long-Term Optimization of Cogeneration Systems in a Competitive Market Environment", *Applied Energy*, Vol. 81, pp. 152-169.